PSVue®: Novel small molecule probes for fluorescent imaging of apoptosis and bacterial infections *in vitro* and *in vivo*

PSVue® has been developed by Molecular Targeting Technologies, Inc. (MTTI) as a robust alternative to probes currently used by researchers to detect early-to-mid stage apoptosis, as well as bacterial infections. PSVue® functions similarly to Annexin-V protein by binding to phosphatidylserine (PS) biomarkers on diseased cell surfaces. PSVue® is also capable of binding to and detecting anionic phospholipids on the surfaces of bacterial cell envelopes. PSVue® is more cost-effective than most Annexin analogs, and it is compatible with many current imaging techniques such as fluorescent microscopy and flow cytometry.

The PSVue® product family of fluorescent imaging reagents is based upon the positively charged bis(zinc-dipicolylamine) (Zn-DPA) chemical structure (Smith, Bradley; US Patent 7,179,616; licensed by MTTI) that functions as an Annexin-V mimic by targeting exposed anionic phospholipids such as phosphatidylserine on plasma membranes. It binds with high selectivity to the surfaces of apoptotic and necrotic cells which contain exposed PS on their membranes, and is therefore well suited for researchers studying *in vitro* or *in vivo* processes involving excessive or insufficient cell death. These may include cancer, neurological disorders, cardiovascular diseases, and tissue damage. PSVue® is also capable of detecting and imaging anionic phospholipids on the surfaces of Gram-positive and Gram-negative bacterial cell envelopes.

PSVue® is expected to possess a number of advantages over Annexin-V compounds which are used to detect PS exposure during apoptosis. These may include:

- Binding kinetics are fast; Annexin-V binding is slow
- Binding is Ca^{2+} independent; no artifacts due to activation of nonspecific membrane scramblases by Ca^{2+}
- Cheaper synthesis and greater stability, compared to most Annexin-V fluorescent analogs
- Apoptosis can be detected under a wide variety of conditions (e.g. in presence of 10% serum, temperatures from 4 to 37^{o}C)
- PSVue® probes can provide more intense labeling due to their much smaller size (i.e. >10 PSVue® molecules can bind to the same area as 1 Annexin-V molecule)

Figure 1 depicts a generalized structure and mechanism of action of PSVue® probes. The PSVue® probe consists of an organic scaffolding which coordinates two positively-charged Zn^{2+} ions to form a complex (the "affinity group"). The organic component is conjugated, via a chemical linker, to a reporter group which is a fluorescent moiety[1]. Zn^{2+} then induces strong association of the complex through electrostatic interactions with carboxylate and phosphate anions present in the PS headgroup of dead and dying cell membranes, in turn leading to fluorescent labeling of the target bearing exposed PS[2]. PSVue® has been found to be highly selective for phosphatidylserine on vesicle membranes, compared to other species of phospholipids[3].

PSVue® reagent kits are differentiated by means of the available absorption and emission wavelength spectra of the reporter group. These include PSVue® 794 (Cy7/Near-Infrared analog), PSVue® 380 (Anthracene analog), PSVue® 480 (FITC analog), PSVue® Biotin (Biotin analog) and PSVue® 550 (Rhodamine analog). PSVue® reagents are useful for *in vitro* and *in vivo* research applications in that they allow for concurrent multiple wavelength detection from long-UV to near-infrared, and are compatible for use with most imaging equipment for fluorescence microscopy and flow cytometry. The use of these reagents is also envisioned in high-throughput screening of drug candidates, automated cell culture screening or *in vitro* diagnostic testing in oncology or bacteriology.

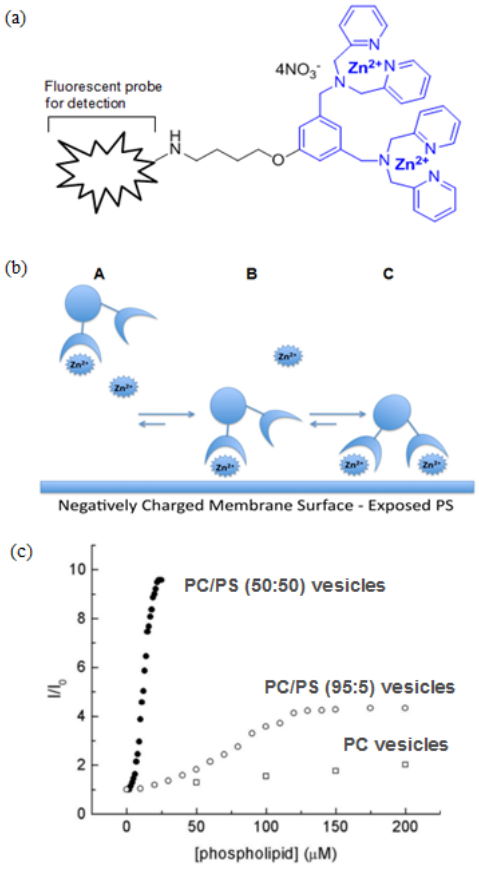

Figure 1: Structure and mechanism of action of PSVue® fluorescent probes
(a) Schematic diagram of PSVue® probes
(b) Mechanism of binding of PSVue® to cell surface containing anionic phospholipids
(c) Change in fluorescence intensity I/I_0 (ex 380, em 440 nm) of PSVue® 380 (1 mM) in HEPES buffer (10 mM, pH 7.2) upon addition of 100 nM unilamellar vesicles composed of POPC : POPS (50 : 50, filled circles), POPC : POPS (95 : 5, open circles), 100% POPC (squares).

Diagrams published by Smith *et al*., *Israel J. Chem*, **45**, 2005[2] and Smith *et al*., *Cell Death Differ.*, **10(12)**, 2003[3].

PSVue® for *in vitro* cell death detection

Figure 2a depicts the utility of PSVue® as a tool for *in vitro* staining applications[1]. For instance, *in vitro* fluorescence microscopy tests using Annexin-V and PSVue® biotin (100 μM) with a blue-emitting streptavidin–dye conjugate (400 nM) have demonstrated that Jurkat cells which were induced to undergo apoptosis using a chemotherapeutic agent (10 uM camptothecin for 3.5h) displayed the same staining pattern when both probes were used simultaneously. In addition, necrotic cells could be differentiated from apoptotic cells via staining with the DNA intercalator 7-aminoactinomycin D (500 ng/ml 7-AAD), which enters necrotic cells due to the disruption of the plasma membrane. On the other hand, cells stained only with Annexin-V or PSVue® biotin and which excluded 7-AAD were in early-to-intermediate stages of apoptosis. These results highlight the ability of PSVue® to identify apoptotic cell populations with the aid of a suitable necrosis-detection agent. This may be useful, for instance, in assessing the effectiveness of treating tumor cell lines with apoptosis-inducing agents *in vitro*. Figure 2b illustrates the use of PSVue® in flow cytometry applications, in which Jurkat cells have been stained by PSVue® 480 and 7AAD[1]. Both control and treated cells exhibit similar levels of staining by 7AAD, indicating that there is the same level of necrotic cells in the population (less than 5□% in each case). Cells treated with camptothecin exhibit significantly more staining by PSVue® 480 than do control cells. Approximately 30□% of treated cells were identified as apoptotic by using PSVue® 480, while less than 5□% of the untreated cells were stained with PSVue® 480.

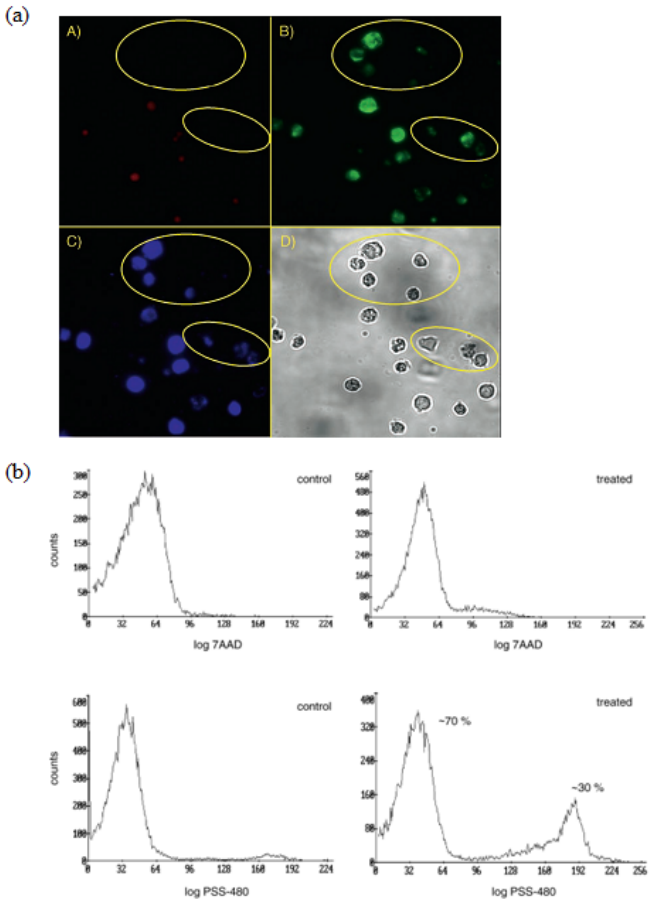

Figure 2: (a) Fluorescence micrographs (40× magnification) of Jurkat cells treated with 10 μM camptothecin for 3.5 h and stained with (A) the nuclear stain 7AAD; (B) Annexin V-FITC; (C) PSVue®-biotin/streptavidin–Marina Blue conjugate (460 nm emission); (D) Bright-field image of the entire field of cells. Cells in the circled regions of each image are apoptotic. No staining of healthy cells was observed in the absence of treatment with camptothecin. All reagents were added simultaneously. Cells were then incubated for 15 min at 37□°C.
(b) Flow-cytometry graphs illustrating staining of Jurkat cells by PSVue® 480 and 7AAD.

Diagrams published by Smith *et al.*, *ChemBiochem*, **6**, 2005[1].

PSVue® for *in vivo* targeting and imaging of cell death

A fluorescent near-infrared (NIR) conjugate of Zn-DPA (PSVue® 794) has been shown to localize to and image cell death in animal models induced by a variety of chemically-acting agents. Smith *et al.*[4] demonstrated the utility of PSVue® 794 for detecting acute cell death and tissue damage induced by (a) A synthetic ionophore, (2) Ethanol, a moderate cytotoxic agent, and (3) Ketamine (Figures 3 and 4). Further, a comparative study with the commercially available NIR fluorescent conjugate Annexin Vivo-750 (VisEn Medical) showed less intense uptake for the latter compound at the site of muscle damage, and high accumulation in the bladder (Figures 5 and 6). In a separate study, rats were treated with dexamethasone to induce thymic atrophy, with thymus uptake of PSVue® 794 being four times higher than a control fluorophore that lacked the Zn-DPA affinity ligand. While PSVue® 794 cleared more rapidly through the liver/intestines, Annexin V cleared primarily via the bladder. The signal intensity of PSVue® 794 was also shown to correlate with that of the expression of caspase-3 when dexamethasone-treated rat thymi were studied with both PSVue® 794 and anti-caspase staining (Figures 7 and 8)[5]. A maximum of signal intensity was achieved at 42h post dexamethasone treatment when both anti-caspase staining and PSVue® 794 were used simultaneously, but a maximum was attained at 12 h when only anti-caspase staining was used. A possible explanation is that the presence of PSVue® 794 causes a delayed and higher build up of dead and dying cells in the rat thymus, suggesting its ability to modulate the rate of clearance of these cells by phagocytosis. Hence, PSVue® 794 may serve as a complementary probe to existing alternatives for imaging cell death at different anatomical locations (Annexin V, different route of clearance limits imaging locations), or at different time points (different signal maxima for PSVue® and caspase staining).

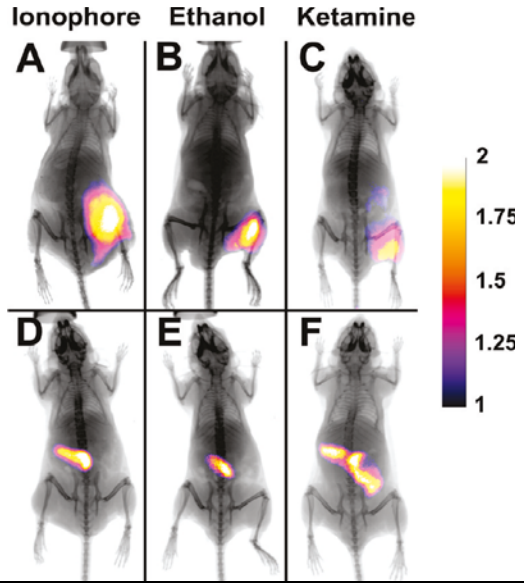

Figure 3: X-ray and fluorescence overlay images of mice treated with either synthetic ionophore 1, ethanol, or ketamine and dosed with PSVue® 794 (A-C) or 794-control probe which does not contain the PS targeting moiety (D-F). Images were acquired 24 h post-injection of the probes. The calibration bar shows the fold increase in fluorescence counts from the minimum fluorescence counts. Diagrams published by Smith *et al*., *Mol. Pharm.*, **8(2)**, 2011[4].

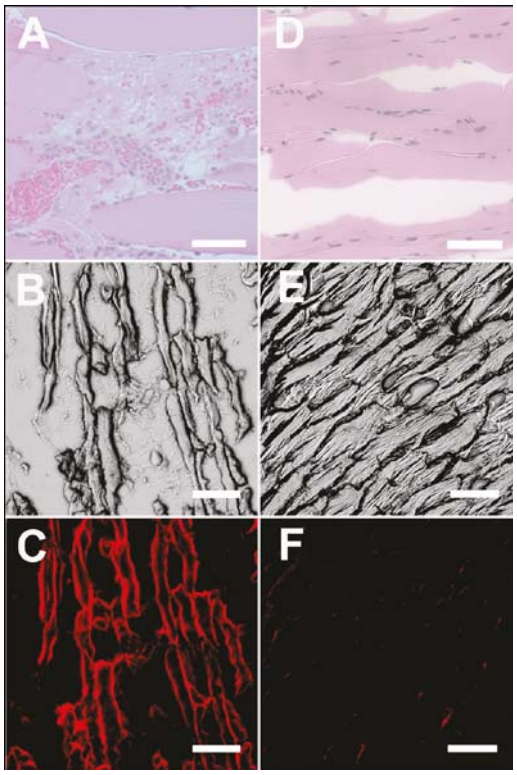

Figure 4: Representative histological sections from damaged leg muscle due to injection of ionophore 1 (A-C) or undamaged leg muscle that was only injected with saline (D-F). The micrographs were subjected either to H&E staining (A, D) or left unstained. Unstained micrographs were viewed using the brightfield (B, E) and NIR (C, F) filter sets. Scale bar = 200 μm for panels A and D. Scale bar = 50 μm for panels B, C, E, F. Diagrams published by Smith *et al*., *Mol. Pharm.*, **8(2)**, 2011[4].

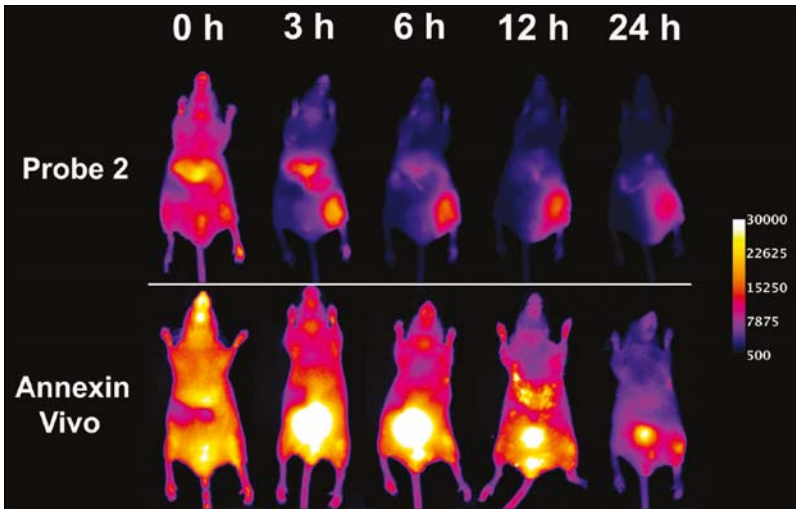

Figure 5: Representative NIR fluorescence images of a mouse treated with ionophore 1 in the hind leg and injected with either PSVue® 794 (top row) or Annexin-Vivo 750 (bottom row) via the tail vein. Both cohorts of mice were injected with ionophore 1 in the right hind leg muscle and saline in the left hind leg muscle. The mice were dosed with either probe 2 or Annexin-Vivo 750 two hours post-treatment. Images were acquired at the indicated time points after probe injection. The calibration bar applies to all images. Diagrams published by Smith *et al*., *Mol. Pharm.*, **8(2)**, 2011[4].

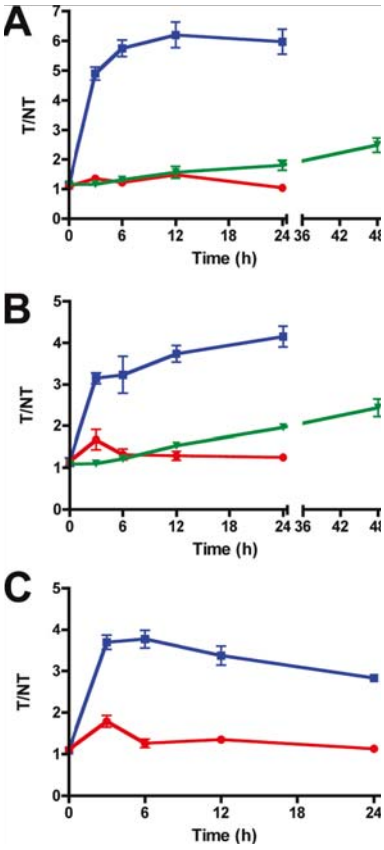

Figure 6: Target/Nontarget (T/NT) ratios of PSVue® 794 (blue), 794-control (green), and Annexin- Vivo 750 (red) in ionophore (A), ethanol (B), and ketamine (C) treated mice. T/NT ratios were calculated at each time point for each cohort tested. Error bars represent the standard error of the mean. N = 4, except n = 3 for probe 2 in B. $P < 0.006$ for PSVue® 794 vs 794-control in A. $P < 0.01$ for PSVue® 794 vs 794-control in B and C. Diagrams published by Smith *et al*., *Mol. Pharm.*, **8(2)**, 2011[4].

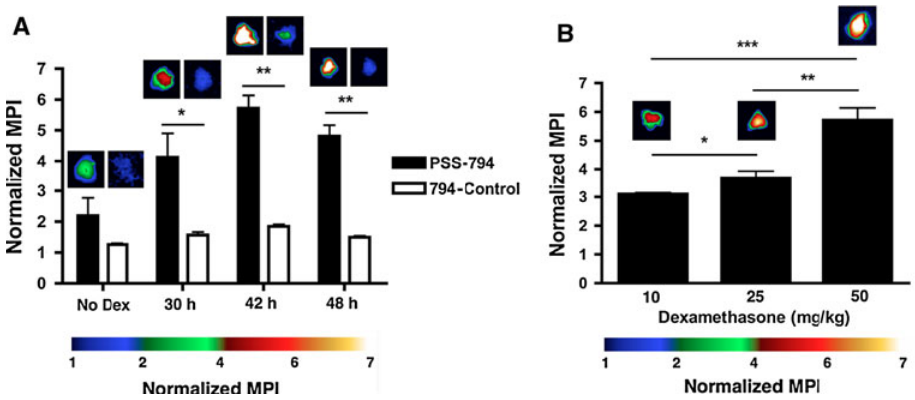

Figure 7: PSVue® 794 selectively targets thymocyte cell death in dexamethasone- treated rats. (a) Mean pixel intensities (MPI) of excised thymi from rats that were treated with dexamethasone (50 mg/kg) and dosed with either PSVue®794 or 794-control (3.0 mg/kg). The times indicate the period from dexamethasone treatment to sacrifice and include injection of the fluorescent probe at 24 h before sacrifice. Rats not treated with dexamethasone (No Dex) were dosed with either PSVue® 794 or 794-control (3.0 mg/kg) and sacrificed 24 h later. In each case, the Mean Pixel Intensity (MPI) for the excised thymus was normalized to the MPI for the heart tissue. Mean ± SEM. N = 4. * P\0.01, ** P\0.0001. (b) Accumulation of PSVue® 794 in the excised thymi depends on the dexamethasone dose size. *Ex vivo* fluorescence images and quantification of MPI were performed 42 h after treatment with dexamethasone. Mean ± SEM. n = 4. * P\0.05, ** P\0.005, *** P\0.001. Diagrams published by Smith *et al*., *Apoptosis*, **16(7)**, 2011[5].

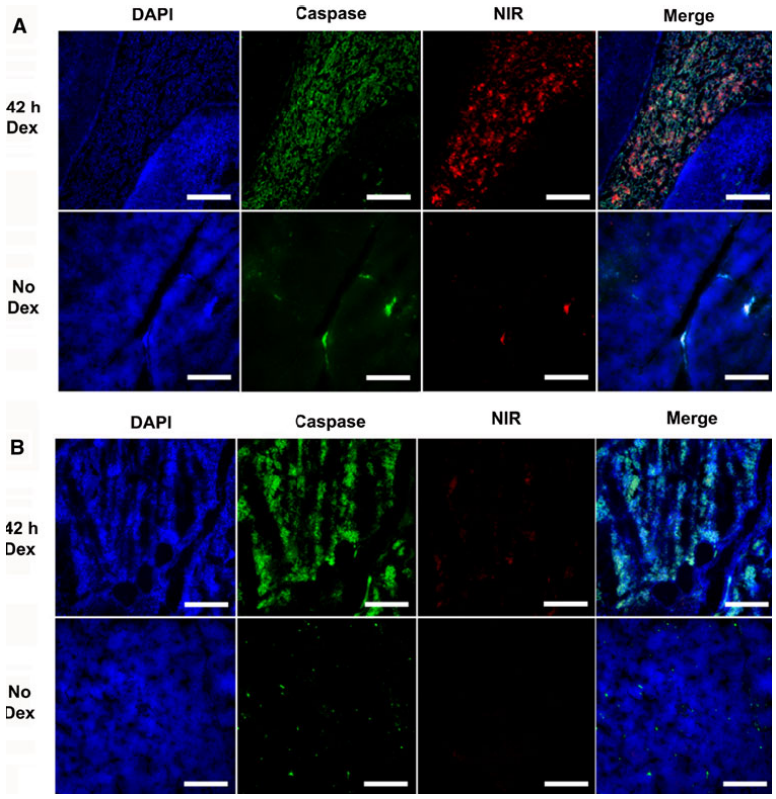

Figure 8: Fluorescence microscopy of thymus histological sections from rats that were treated or not treated with dexamethasone. Rats were treated with dexamethasone (50 mg/kg) and sacrificed 42 h later, with a dose of either (a) PSVue® 794 or (b) 794-control delivered at 24 h before sacrifice. Rats not treated with dexamethasone (No Dex) were dosed with either PSVue® 794 or 794-control (3.0 mg/kg) and sacrificed 24 h later. The 10 l m thick sections were counterstained with DAPI and anti-caspase-3 antibody. The near-infrared (NIR) image in a shows PSVue® 794 targeting regions of tissue containing high levels of caspase-3 due to dexamethasone treatment, whereas, the NIR image in b shows negligible accumulation of 794-control. Scale bar = 200 l m. Diagrams published by Smith *et al*., *Apoptosis*, **16(7)**, 2011[5].

PSVue® for cancer imaging and monitoring of therapeutic intervention

Smith *et al.*[6] have demonstrated that Zn-DPA is capable of selectively targeting anionic dead and dying cells within the necrotic cores of EMT-6 mammary and PAIII prostate xenograft tumors in rat and mouse models, respectively (Figure 9). A 3.0 mg/kg dose of PSVue® 794 demonstrated selective accumulation in the rat prostate and mouse mammary tumors 24 hrs post-injection of probe, with significant target/non-target (T/NT) fluorescent signal ratios and better target accumulation than control probes. In comparing PSVue® to the probe controls, there was a 36-fold increase in tumor targeting for the prostate tumor model, and a 70% higher T/NT ratio than for control for the mammary tumor model. These studies demonstrate the potential of PSVue® 794 to non-invasively detect tumors in animal models, given the ability of near-infrared light to penetrate well through skin and tissue. It may also be possible to use PSVue® 794 to monitor tumor cell death induced by anticancer therapies *in vivo*.

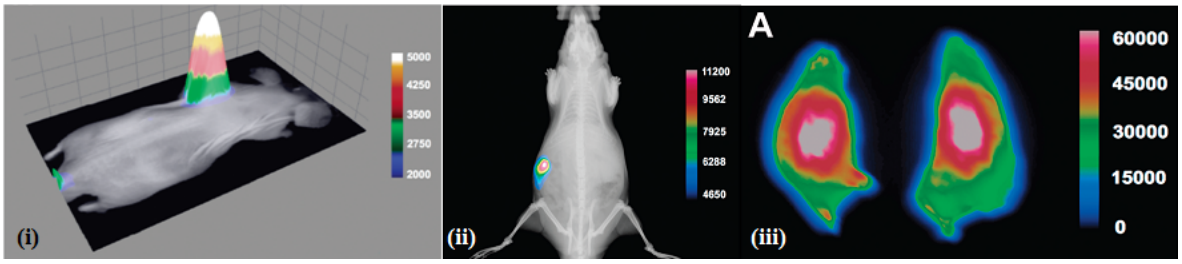

Figure 9: (i) Representative overlay image of a nude mouse with an EMT-6 mammary tumor. Brightfield and fluorescence intensity images were acquired 24 h following injection of PSVue® 794 probe (ii) X-ray and fluorescence overlay image of a rat prostate tumor model at 24 h postinjection of probe. Ex vivo analysis of probe 1 localization in rat prostate tumor. (iii) Excised PAIII prostate tumors were sliced along the longest axis, and a 30 mm field of view generated the representative near-IR fluorescence intensity image. Diagrams published by Smith *et al.*, *J. Am. Chem. Soc.*, **132(1)**, 2010[6].

PSVue® 794 also demonstrates utility in monitoring cell death induced in tumors following radiation treatment *in vivo* (Figure 10)[5]. 6-day old rear leg tumors were induced in rat models and irradiated with 20 Gy of focal beam radiation, and PSVue® 794 or 794-control were injected 17 h after radiation. The amount of PSVue® 794 in the radiation- treated tumor was almost twice that in the non-treated tumor and approximately 8 fold higher than the amount of 794-control in a treated tumor. Furthermore, uptake of 794-control in the radiation-treated tumor was the same as the non-treated tumor. PSVue® 794 also accumulated in the liver, kidneys, and lungs, as seen in tumor bearing rats that were not treated with radiation.

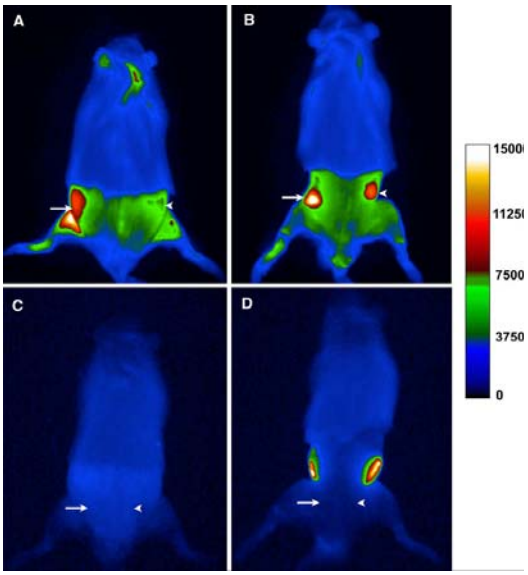

Figure 10: Representative planar, epifluorescence images of rats bearing two subcutaneous PAIII prostate tumors and dosed with PSVue® 794 (a *in vivo*, b *ex vivo*) or 794-control (c *in vivo*, d *ex vivo*) after radiation therapy. The right flank tumor (arrow) received focal beam radiation therapy, and the left flank tumor (arrow head) was not treated. At 17 h after radiation, each rat was injected intravenously with probe (3.0 mg/kg), and 24 h later the in vivo image was acquired. The rats were then sacrificed, the lower body skin removed, and the *ex vivo* image was acquired. The 794-control does not target the tumors but accumulates in the kidneys. n = 5. Diagrams published by Smith *et al.*, *Apoptosis*, **16(7)**, 2011[5].

PSVue® for bacteria imaging

Within the scope of bacteriology, a Zn-DPA probe containing a deep-red squaraine rotaxane reporter dye enabled strong fluorescent imaging of various Gram-positive and Gram-negative bacterial genera including cultures of *S. aureus*, *E. coli*, *S. enterica* serovar typhimurium AM3, *P.aeruginosa*, *K. pneumoniae* and *P. vulgaris*. (10μM probe against ~10^8 CFU of bacteria)[7], and allows for the monitoring of bacterial division by binary fission (Figure 11)[8]. In addition, Zn-DPA was shown to target bacterial infection (*S. aureus* NRS11), but not sterile inflammation in immunocompetent mice[7] (Figure 12). Selective targeting of bacterial infection *in vivo* could be achieved 12 hrs post-injection of probe, and gave T/NT ratios that were 3 times higher than T/NT ratios achieved with administration of an inflammation-inducing agent (1% λ-carrageenan solution). These results suggest the usefulness of Zn-DPA fluorescence imaging as a convenient alternative to commonly used bioluminescent imaging of bacteria, which necessitates time-consuming incorporation of genetic reporters into bacteria and whose signal is dependent on local ATP and oxygen levels. Moreover, Zn-DPA being a wide-spectrum bacterial probe serves as a useful complement in situations where bioluminescence imaging has its limitations.

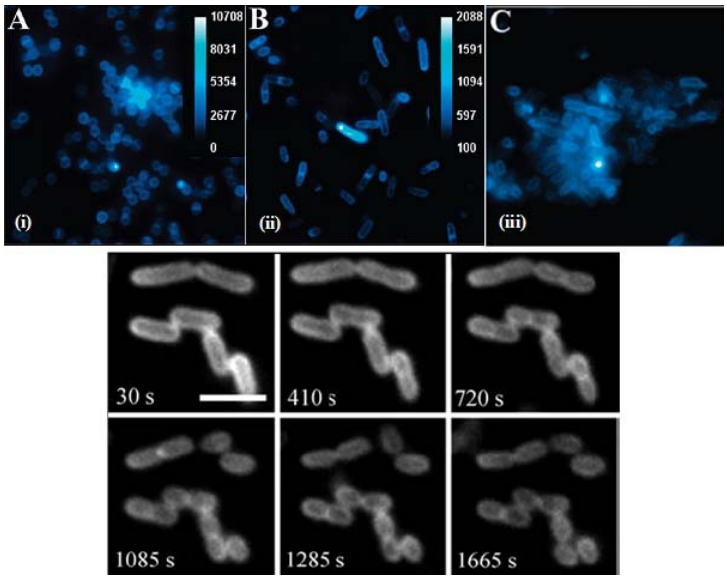

Figure 11: Epifluorescence microscopy of (i) planktonic *S. aureus* NRS11, (ii) *S. enterica* serovar *typhimurium* AM3, and (iii) *E. coli* K12 after incubation of ~10^8 CFU with Zn-DPA NIR probe (10 μM). Images viewed at 1500× magnification and show pixel intensity with scale bar in arbitrary units. (Bottom panel): Binary fission of *E. coli* cells stained with Zn-DPA NIR probe. The cells were imaged every 5 s for 30 min by using fluorescence microscopy. The times stated in each panel correspond to the movie time point and the scale bar represents 2 mm. Diagrams published by Johnson et al., *Angew. Chem. Int. Ed.*, **46**, 2007[7] and White *et al.*, *Bioconjug Chem.*, **21(7)**, 2010[8]

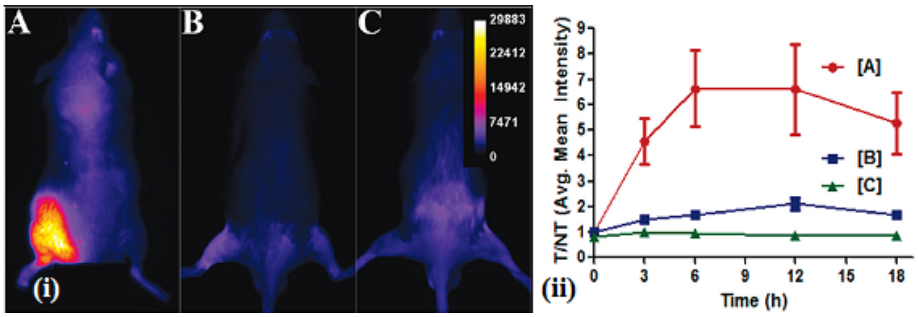

Figure 12: (i) A Zn-DPA deep-red squaraine rotaxane probe targets bacterial infection and not sterile inflammation in immunocompetent mice (strain ICr). (A) Mice were treated with 10 nM of probe six hours after the left posterior leg was injected with ~10^8 CFU of *S. aureus* NRS11, (B) 50 µL of a 1% λ-carrageenan solution, or (C) 50 µL of a sterile saline solution. The dorsal images were acquired at 12 h post injection of probe. (ii) Graph depicts the change in target-to-nontarget ratios (T/NT) obtained via ROI analyses of images. Error bars represent standard error of the mean. N= 3 for each group.
Diagrams published by White *et al.*, *Bioconjug Chem.*, **21(7)**, 2010[7].

An alternative means by which Zn-DPA may image bacterial infections has been proposed by Thakur *et al.*[9]. A near-infrared probe PSVue® 794 was used to image pyogenic abscesses induced by a combination of three strains of bacteria in a mouse infection model: *Escherichia coli*, (gram-negative, ATCC-25922), *Enterococcus faecalis* (gram-positive, ATCC-29212), and *Staphylococcus lugdunensis* (gram-positive, ATCC- 29213), as well as turpentine-induced sterile inflammation. At 3 hr post injection, the lesion to background intensity ratios in the foci of infection (6.6±0.2), were greater than that in the foci of inflammation (3.1±0.5) (Figure 13). *Ex vivo* labeling of human-derived apoptotic neutrophils which is associated with the resolution of infection has been observed with PSVue® 794 (Figure 14), and was proposed to provide a significant contribution towards the fluorescent imaging observed with *in vivo* bacterial infections in mouse models.

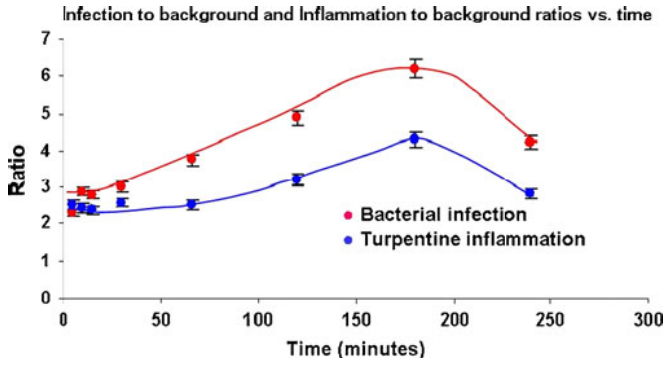

Figure 13: Bacterial infection to background and turpentine-induced inflammation to background image intensity ratios (averaged n=5 each) plotted as a function of time after the administration of the fluorophore. Diagrams published by Thakur *et al.*, *Mol. Imaging Biol.*, 2011[9].

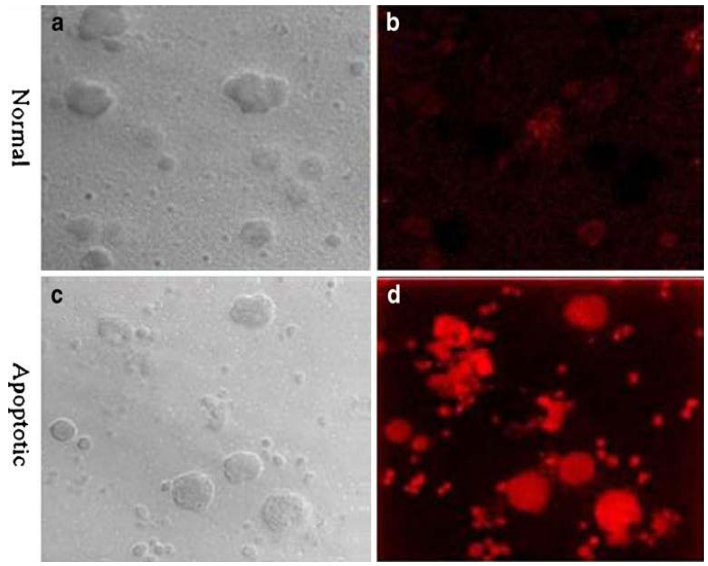

Figure 14: Confocal microscopic images of (a) normal and (b) PSVue® 794-incubated normal white blood cells. Apoptotic white blood cells (c) with intense PSVue® 794 fluorescence specific for phosphatidylserine (d) (×63). Diagrams published by Thakur *et al.*, *Mol. Imaging Biol.*, 2011[9].

In summary, MTTI's Zn-DPA reagents have demonstrated efficiency and are widely applicable to the optical imaging of a variety of disease indications such as cancer, bacterial infections, and tissue damage. These reagents may also have potential in targeting and imaging a range of cardiology and neurological diseases involving cell death. PSVue® is expected to be a cost-efficient and molecularly flexible compound that is customizable to research, industry or clinical applications. Information on PSVue reagent kits is available at http://www.mtarget.com/mtti/psvue.html.

References

1. Hanshaw, R.G., Lakshmi, C., Lambert, T.N., Johnson, J.R. and Smith, B.D. Fluorescent detection of apoptotic cells by using zinc coordination complexes with a selective affinity for membranes surfaces enriched with phosphatidylserine. *ChemBioChem*, **6**, 2214-2220 (2005).

2. Koulov, A.V., Hanshaw, R.G., Stucker, K.A., Lakshmi, C., Smith, B.D. Biophysical studies of a synthetic mimic of the apoptosis-detecting protein Annexin V. *Israel J. Chem*, **45**, 373-379 (2005).

3. Koulov, A.V., Stucker, K.A., Lakshmi, C., Robinson, J.P., Smith, B.D. Detection of apoptotic cells using a synthetic fluorescent sensor for membrane surfaces that contain phosphatidylserine. *Cell Death Differ.*, **10(12)**, 1357-1359 (2003).

4. Smith, B. A., Gammon, S. T., Xiao, S., Wang, W., Chapman, S., McDermott, R., Suckow, M.A., Johnson, J. R., Piwnica-Worms, D., Gokel, G. W., Smith, B. D., Leevy, W. M. *In Vivo* Optical Imaging of Acute Cell Death Using a Near-Infrared Fluorescent Zinc-Dipicolylamine Probe. *Mol. Pharm.*, **8**, 583-590 (2011).

5. Smith, B. A., Xiao, S., Wolter, W., Wheeler, J., Suckow, M. A., Smith, B. D. *In Vivo* Targeting of Cell Death Using a Synthetic Fluorescent Molecular Probe. *Apoptosis*, **16**, 722-731 (2011).

6. Smith *et al*. Optical imaging of mammary and prostate tumors in living animals using a synthetic near infrared zinc(II)-dipicolylamine probe for anionic cell surfaces. *J. Am. Chem. Soc.*, **132(1)**, 67-69 (2010).

7. White *et al*. Optical imaging of bacterial infection in living mice using deep-red fluorescent squaraine rotaxane probes. *Bioconjug Chem.*, **21(7)**, 1297-1304 (2010).

8. Johnson, J. R., Fu, N., Arunkumar, E., Leevy, W. M., Gammon, S. T., Piwnica-Worms, D., Smith, B. D. Squaraine-Rotaxanes: Superior Substitutes for Cy-5 in Molecular Probes for Near-Infrared Fluorescence Cell Imaging. *Angew. Chem. Int. Ed.*, **46**, 5528-5531 (2007).

9. Thakur, M.L., Zhang, K., Paudyal, B., Devakumar, D., Covarrubias, M.Y., Cheng, C.P., Gray, B., Wickstrom, E., Pak, K.Y. Targeting Apoptosis for Optical Imaging of Infection. *Molecular Imaging and Biology*, 2012, 14, 163-171.

Miscellaneous Publications

1. Lakshmi, C., Hanshaw, R. G., Smith, B. D. Fluorophore Linked Zinc (II) Dipicolylamine Coordination Complexes as Sensors for Phosphatidylserine Containing Membranes. *Tetrahedron*, **60**, 11307-11315 (2004).

2. Hanshaw, R. G., O'Neil, E. J., Foley, M., Carpenter, R. T., Smith, B. D. Indicator Displacement Assays that Detect Bilayer Membranes Enriched in Phosphatidylserine. *J. Materials Chem.*, **15**, 2707 – 2713 (2005).

3. Hanshaw, R. G., Smith, B. D. New Reagents for Phosphatidylserine Recognition and Detection of Apoptosis. *Bioorg. Med. Chem.*, **13**, 5035-5042 (2005).

4. Leevy, W. M., Johnson, J. R., Lakshmi, C., Morris, J., Marquez, M., Smith, B. D. Selective Recognition of Bacterial Membranes by Zinc(II)-Coordination Complexes. *Chem. Comm.*, 1595-1597 (2006).

5. Leevy, W. M., Gammon, S. T., Jiang, H., Johnson, J. R., Maxwell, D. J., Marquez, M., Piwnica-Worms, D., Smith, B. D. Optical Imaging of Bacterial Infection in Living Mice Using a Fluorescent Near-Infrared Molecular Probe. *J. Am. Chem Soc.*, **128**, 16476-16477 (2006).

6. DiVittorio, K. M., Johnson, J. R., Johansson, E., Reynolds, A. J., Jolliffe, K. A., Smith, B. D. Synthetic Peptides with Selective Affinity for Apoptotic Cells. *Org. Biomol. Chem.*, **4**, 1966 – 1976 (2006).

7. DiVittorio, K. M., Leevy, W. M., O'Neil, E. J., Johnson, J. R., Vakulenko, S., Morris, J. D. Rosek, K. D., Serazin, N., Hilkert, S., Hurley, S., Marquez, M., Smith, B. D. Zinc(II)-Coordination Complexes as Membrane Active Fluorescent Probes and Antibiotics. *ChemBiochem*. **9**, 286-293 (2008).

8. Johnson, J. R., Jiang, H., Smith B. D. Zinc (II)-Coordinated Oligotyrosiine: A New Class of Cell Penetrating Peptide. *Bioconj. Chem.*, **19**, 1033-1039 (2008). **Chosen by editor as the cover article.**

9. Leevy, W. M., Gammon, S. T., Johnson, J. R., Lampkins, A. J., Jiang, H., Marquez, M., Piwnica-Worms, D., Smith, B. D. Non-Invasive Optical Imaging of *Staphylococcus aureus* Bacterial Infection in Living Mice Using a Bis-Dipicolyamine-Zinc(II) Affinity Group Conjugated to a Near Infrared Fluorophore. *Bioconj. Chem.* **19**, 686-692 (2008).

10. Leevy, W. M., Lambert, T. N., Johnson, J. R., Morris, J., Smith, B. D. Quantum Dot Probes for Bacteria Distinguish *Escherichia coli* Mutants and Permit *In Vivo* Imaging. *Chem. Comm.*, **20** 2331-2333 (2008). **Highlighted by the journal as a Hot Paper.**

11. Hope-Roberts, M., Wainwright, M., Horobin, R.W. Real Time Imaging of Bacteria in Living Mice Using a Fluorescent Dye. *Biotech. Histochem.*, **86(2)**, 104-107 (2011).

12. Baumes, J. M., Gassensmith, J. J., Giblin, J., Lee, J.-J., White, A. G., Culligan, W. J., Leevy, W. M., Kuno, M., Smith, B. D. Storable, Thermally Activated, Near-Infrared Chemiluminescent Dyes and Dye-Stained Microparticles for Optical Imaging. *Nature Chem.*, **2**, 1025-1030 (2010).

13. Kaimal, V., Chu, Z., Mahller, Y.Y., Papahadjopoulos-Sternberg, B., Cripe, T.P., Holland, S.K., Qi, X. Saposin C Couple Lipid Nanovesicles Enable Cancer-Selective Optical and Magnetic Resonance Imaging. *Mol. Imaging Biol.* (2010). Epub ahead of print.

14. Niu, G., Chen, X. Apoptosis Imaging: Beyond Annexin V. J. Nucl. Med., **51(11)**, 1659-1662 (2010).

15. Wyffels, L., Gray, B., Barber, C., Pak, K., Forbes, S., Mattis, J., Woolfenden, J., Liu, Z. Detection of myocardial ischemia-reperfusion injury using a fluorescent near-infrared zinc(II)-dipicolylamine probe and ^{99m}Tc-glucarate. *Mol. Imaging Biol.* (2011).

16. Wyffels, L., Gray, B., Barber, C., Pak, K., Woolfenden, J., Liu, Z. Synthesis and preliminary evaluation of radiolabeled bis(zinc(II)–dipicolylamine)coordination complexes as cell death imaging agents. *Bioorg. Med. Chem.*, **19**, 3425–3433 (2011).

17. Liu X, Cheng D, Gray BD, Wang Y, Akalin A, Rusckowski M, Pak KY, Hnatowich DJ. Radiolabeled Zn-DPA as a potential infection imaging agent. Nucl Med Biol. 2012 Feb 7 (epub ahead of print)

18. Li J., Gray B., Pak KY., Ng CK. J Optimization of labeling dipicolylamine derivative, N,N'-(5-(4-aminobutoxy)-1,3-phenylene)bis(methylene)bis(1-(pyridin-2-yl)-N-(pyridin-2-ylmethyl)methanamine), with three 18F-prosthetic groups as potential imaging agents for metastatic infectious disease. Labelled Compounds and Radiopharmaceuticals 2012; in press.

19. White A, Gray BD, Pak KY, Smith BD. Deep-red fluorescent imaging probe for bacteria. Bioorganic and Medicinal Chemistry Letters. 2012; in press

Website: http://www.mtarget.com/mtti/psvue.html

Corresponding Author

Dr Brian Gray, Ph.D.
VP Research, Molecular Targeting Technologies, inc.
833 Lincoln Avenue, Unit 9, West Chester, PA 19380
Phone: +1 610 738 7938
Fax: +1 610 738 7928
E-mail: briangray@mtarget.com